11th World Congress on Computational Mechanics (WCCM XI)
5th European Conference on Computational Mechanics (ECCM V)
6th European Conference on Computational Fluid Dynamics (ECFD VI)
E. Oñate, J. Oliver and A. Huerta (Eds)

MICRO-MECHANICAL MODELING OF DUCTILE DAMAGE AND FAILURE TAKING INTO ACCOUNT VARIOUS STRESS-STATES

VANESSA HAGENBROCK*, STEFFEN GERKE* AND MICHAEL BRÜNIG*

*Institut für Mechanik und Statik
Universität der Bundeswehr München
Werner-Heisenberg-Weg 39, 85577 Neubiberg, Germany
e-mail: vanessa.hagenbrock@unibw.de, web page: https://www.unibw.de/baumechanik/

Key words: Ductile materials, Damage and fracture, Stress triaxiality, Lode parameter, Micro-mechanical numerical simulations

Abstract. The paper discusses the effect of stress state on plastic deformations, damage mechanisms and fracture of ductile materials. To be able to model these various effects a continuum damage model has been generalized to take into account the dependence on stress-state on the constitutive approach. The model is based on the introduction of damaged and fictitious undamaged configurations. Different branches are used corresponding to various damage mechanisms depending on stress intensity, stress triaxiality and the Lode parameter. It is nearly impossible to identify all constitutive parameters only by experiments. Therefore, to get more insight in the complex damage mechanisms aditional series of three-dimensional micro-mechanical simulations of void containing unit cells have been performed. They cover a wide range of stress triaxialities and Lode parameters in tension, shear and compression domains. Furthermore, these numerical results are used to propose the damage equations and to identify corresponding parameters.

1 INTRODUCTION

Accurate and realistic material models describing inelastic behavior, damage and fracture of ductile metals are evident in computational and structural mechanics. They are used in engineering applications and become more and more important in numerical analyses of structural components and in assessment of structural reliabilty. As a result a large number of continuum damage approaches as well as associated efficient algorithms have been discussed in the literature. However, damage is present in many ductile materials, increase with inelastic deformations and leads to final failure of the engineering structures. The continuum theories taking into account these effects model in a phenomenological way growth and coalescence of micro defects. Furthermore they describe

corresponding macroscopic material softening during damage and fracture processes under general loading conditions. Critical internal scalar or tensorial damage variables are used to characterize the onset of damage.
It has been discussed during the last years that the stress state remarkably influences the damage and failure mechanisms. Thus, the stress intensity, the stress triaxiality and the Lode parameter are important factors to characterize the onset and evolution of ductile damage and failure. To analyze these effects experiments and corresponding numerical simulations have been performed. They take into account series of tests with differently designed and loaded specimens to cover a wide range of stress states [1, 2, 3, 4, 5, 6, 7].
With today's computational technique it is not possible to analyze deformation behavior of structures describing damage and failure mechanisms on the microscale. Therefore representative volume elements (RVEs) with micro-structural details are used to develop constitutive equations on the macroscopic level [8, 9, 10, 11, 12, 13, 14, 15, 16]. On one hand the rate of expansion of micro-defects in different directions depends on the Lode parameter. On the other hand the results of these micro-mechanical numerical simulations have shown that void growth, macroscopic deformation behavior and the critical failure strain conspicuously depend on the stress triaxiality.
Many authors only consider void growth and coalescence with high hydrostatic stress states. These results are only valid from moderate to high stress triaxialities where the effect of the Lode parameter can be neglected. Therefore, the present paper discusses further micro-mechanical simulations covering a wide range of loading conditions in the tension, shear and compression domains. The results from these numerical unit cell simulations deliver detailed information on damage and failure mechanisms for a wide range of stress states. They are used to propose and to validate the constitutive equations of the continuum damage model and to identify corresponding parameters.

2 CONTINUUM MODEL

The inelastic deformation behavior including anisotropic damage caused by micro-defects and their interactions are described by a phenomenological framework [17]. The model is based on the introduction of damaged as well as fictitious undamaged configurations. It takes into account the additive decomposition of strain rate tensors in elastic, plastic and damage parts. An isotropic hyperelastic law characterizes the elastic behavior and takes into account constant shear and bulk modulus. Furthermore, the plastic behavior has to be described by the Drucker-Prager-type yield condition

$$f^{pl}\left(\bar{I}_1, \bar{J}_2, c\right) = \sqrt{\bar{J}_2} - c\left(1 - \frac{a}{c}\bar{I}_1\right) = 0\,, \tag{1}$$

according to the fact that the plastic behavior is affected by the stress state and that the plastic yielding of the undamaged matrix material depends on the stress triaxiality. In Eq. (1) $\bar{I}_1 = \mathrm{tr}\bar{\mathbf{T}}$ and $\bar{J}_2 = \frac{1}{2}\,\mathrm{dev}\bar{\mathbf{T}}\cdot\mathrm{dev}\bar{\mathbf{T}}$ are invariants of the effective stress tensor $\bar{\mathbf{T}}$, c denotes the strength coefficient of the matrix material and a represents the hydrostatic

stress coefficient of the matrix material where a/c is a constant material parameter. Plastic volumetric strains have been shown to be marginal which leads to the plastic potential function

$$g^{pl}(\bar{\mathbf{T}}) \;=\; \sqrt{\bar{J}_2}\,. \tag{2}$$

Equation (2) depends only on the second invariant of the effective stress deviator resulting in a non-associated isochoric effective plastic strain rate

$$\dot{\bar{\mathbf{H}}}^{pl} \;=\; \dot{\lambda}\,\frac{\partial g^{pl}}{\partial \bar{\mathbf{T}}} \;=\; \dot{\lambda}\,\frac{1}{2\sqrt{\bar{J}_2}}\,\mathrm{dev}\bar{\mathbf{T}} \;=\; \dot{\gamma}\,\bar{\mathbf{N}}\,. \tag{3}$$

In Eq. (3) $\dot{\lambda}$ is a non-negative scalar-valued factor, $\bar{\mathbf{N}} \;=\; (1/\sqrt{2\;\bar{J}_2})\;\mathrm{dev}\bar{\mathbf{T}}$ characterizes the normalized deviatoric tensor and $\dot{\gamma} \;=\; \bar{\mathbf{N}}\cdot\dot{\bar{\mathbf{H}}}^{pl} \;=\; (1/\sqrt{2})\,\dot{\lambda}$ denotes the equivalent plastic strain rate measure used in the constitutive model.

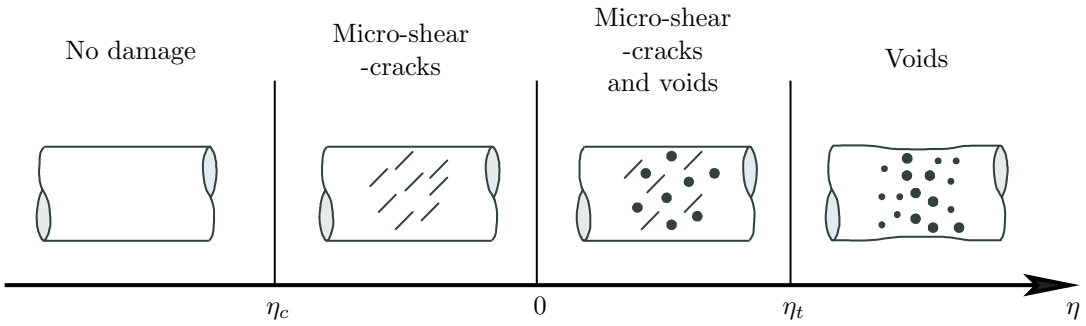

Figure 1: Different damage mechanisms depending on stress triaxiality η

Moreover, to characterize the onset and continuation of damage during further loading of the material a damage criterion is introduced. The damage behavior leading to final fracture depends on different stress triaxialities [2, 16] (see Fig. 1): large stress triaxialities lead to the growth of voids, for negative stress triaxialities the formation of micro-shear-cracks exists and for moderate modes both microscopic mechanisms are present. Furthermore, for large negative stress triaxialities a cut-off value has been proposed. Below this value no further damage and fracture occur [18, 19]. The present investigations take into account the stress triaxiality dependence discussed above and will be generalized by additional regard to the Lode parameter.
As a result, the onset of damage is described by the damage criterion

$$f^{da} = \alpha I_1 + \beta\sqrt{J_2} - \sigma = 0 \tag{4}$$

where α and β denote the stress-state-dependent damage mode parameters depending on the stress intensity $\sigma_{eq} = \sqrt{3J_2}$, the stress triaxiality

$$\eta = \frac{\sigma_m}{\sigma_{eq}} = \frac{I_1}{3\sqrt{3J_2}} \tag{5}$$

as the ratio of the mean stress σ_m and the von Mises equivalent stress σ_{eq} as well as on the Lode parameter

$$\omega = \frac{2\tilde{T}_2 - \tilde{T}_1 - \tilde{T}_3}{\tilde{T}_1 - \tilde{T}_3} \quad \text{with } \tilde{T}_1 \geq \tilde{T}_2 \geq \tilde{T}_3 \tag{6}$$

characterized by the principal stress components $\tilde{T}_1$, $\tilde{T}_2$ and $\tilde{T}_3$. The Lode parameter $\omega = 0$ is associated with shear stress combined with hydrostatic stress, whereas $\omega = \pm 1$ corresponds to axisymmetric stress states: $\omega = -1$ represents uniaxial tension combined with hydrostatic stress while $\omega = +1$ characterizes uniaxial compression combined with hydrostatic stress. In Eq. (4) I_1 and J_2 are the first stress invariant and the second deviatoric stress invariant of the stress tensor in the damaged configurations and σ is the damage threshold. Furthermore a damage evolution law is necessary to describe the increase in macroscopic damage strains. This increase is the consequence of growth of voids, their coalescence and the formation of micro-cracks at the same time:

$$\dot{\mathbf{H}}^{da} = \dot{\mu} \left(\bar{\alpha} \, \frac{1}{\sqrt{3}} \, \mathbf{1} + \bar{\beta} \, \mathbf{N} + \bar{\delta} \, \mathbf{M} \right). \tag{7}$$

The parameters $\bar{\alpha}$, $\bar{\beta}$ and $\bar{\delta}$ are stress-state-dependent variables: $\bar{\alpha}$ characterizes the volumetric, $\bar{\beta}$ and $\bar{\delta}$ correspond to the isochoric damage-based deformations. Furthermore, the parameter $\dot{\mu}$ is the equivalent damage strain rate measure. In addition,

$$\mathbf{N} = \frac{1}{2\sqrt{J_2}} \, \mathrm{dev}\tilde{\mathbf{T}} \tag{8}$$

and

$$\mathbf{M} = \frac{1}{\parallel \mathrm{dev}\tilde{\mathbf{S}} \parallel} \, \mathrm{dev}\tilde{\mathbf{S}} \tag{9}$$

with

$$\mathrm{dev}\tilde{\mathbf{S}} = \mathrm{dev}\tilde{\mathbf{T}} \, \mathrm{dev}\tilde{\mathbf{T}} - \frac{2}{3} \, J_2 \, \mathbf{1} \tag{10}$$

are the normalized stress tensors. Considering all parameters explained above the tensor $\dot{\mathbf{H}}^{da}$ (Eq. 7) models volumetric and deviatoric parts corresponding to isotropic growth of voids and anisotropic evolution of micro-cracks.

3 IDENTIFICATION OF MATERIAL PARAMETERS

Basic material parameters have been identified by experiments and corresponding numerical simulations. For the experiments tension and shear tests with smooth and prenotched specimens taken from aluminum alloys covering different stress triaxialities have to be taken into account. These experiments can be used to identify material parameters in stress-state-dependent plasticity and damage models.
Elastic-plastic material parameters are identified using tension tests with unnotched specimens. The equivalent stress-equivalent strain curves lead to Young's modulus $E = 75000$

MPa and Poisson's ratio is taken to be $\nu = 0.3$. Furthermore, the plastic behavior is characterized by a power law function for the equivalent stress appearing in the yield criterion (1)

$$c = c_0 \left(\frac{H\,\gamma}{n\,c_0} + 1 \right)^n \tag{11}$$

which models the work hardening behavior of the aluminum alloy. Good agreement of experimental and numerical data is achieved with the initial yield strength $c_0 = 250$ MPa, the hardening modulus $H = 3125$ MPa and the hardening exponent $n = 0.135$. Additionally, the hydrostatic stress coefficient in the yield criterion is choosen to be $a/c = 0.00005$ MPa^{-1}. The onset of damage characterized by the damage threshold $\sigma_0 = 325$ MPa appearing in the damage criterion (4) can be identified by using experimental load-engineering strain curves and corresponding numerical analyses of uniaxial tension tests with smooth specimens [7].
As mentioned above the experiments have been performed with flat specimens taken from thin aluminum sheets. Thus, only plane stresses are present and, as a consequence, the effect of the Lode parameter can not be considered. Furthermore it is not possible to identify all parameters appearing in the constitutive equations only by the experiments discussed above. Therefore, additional numerical simulations on the micro-level have been performed to be able to study in detail the appearing mechanisms.

4 NUMERICAL SIMULATIONS ON THE MICRO-SCALE

To get more information about the different stress-state-dependent damage mechanisms micromechanical numerical simulations have been performed. They consider a three-dimensional model of a unit cell with one spherical void (Fig. 2). The behavior of the unit cell, which can be seen as a representative volume element (RVE), with symmetry boundary conditions to model periodic distributions of micro defects under various loading conditions is analyzed in detail. The results from the numerical analyses will be used to identify parameters appearing in the constitutive equations. In this study, the initial porosity of the cell model calculations is 3%. Further analyses with different initial porosities between 1% and 10% as well as initial elliptical voids have not shown remarkably different results as those discussed in this section. For the micro-mechanical numerical simulations the finite element program ANSYS is used. Due to symmetry conditions only one eight of the unit cell is analyzed. The corresponding finite element mesh consists of 3123 3D-elements of type solid185 (Fig. 2). To be able to model various loading conditions a wide range of stress triaxialities and Lode parameters has been taken into account. The principal macroscopic stresses acting on the outer bounds of the RVE and the stress triaxiality coefficient and the Lode parameter are kept constant during the entire loading history of the simulation [16]. Furthermore, the initially plane surfaces have to remain plane during the entire loading history to ensure that the representative volume element can be seen as a part of an initially damaged solid with regular and equidistant

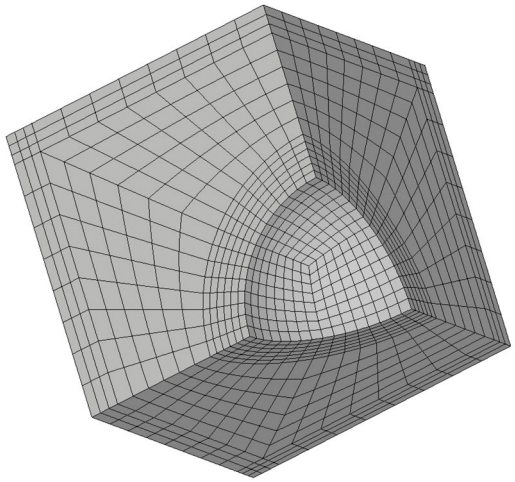

Figure 2: Finite element mesh of one eighth of the unit cell

distribution of spherical voids. Using the results from the numerical analyses it is possible to determine the stress-state-dependent parameters appearing in the damage condition and the damage rule [16]: In particular, the parameters of the damage criterion depending on stress triaxiality η and Lode parameter ω are given by

$$\alpha(\eta) = \begin{cases} 0 \;\; \text{for} \;\; \frac{-1}{3} \leq \eta \leq 0 \\ \frac{1}{3} \;\; \text{for} \;\; \eta > 0 \end{cases} \tag{12}$$

and

$$\beta(\eta,\, \omega) = \beta_0(\eta,\, \omega = 0) + \beta_\omega(\omega) \geq 0 \;, \tag{13}$$

with

$$\beta_0(\eta) = \begin{cases} -0.45\,\eta + 0.85 \;\; \text{for} \;\; \frac{-1}{3} \leq \eta \leq 0 \\ -1.28\,\eta + 0.85 \;\; \text{for} \;\; \eta > 0 \end{cases} \tag{14}$$

and

$$\beta_\omega(\omega) = -0.017\,\omega^3 - 0.065\,\omega^2 - 0.078\,\omega \;. \tag{15}$$

Figure 3 shows that for small stress triaxialities the parameter β becomes dominant. This fact corresponds to the observed damage behavior: dominant shear mechanisms represented by large values of the second deviatoric stress invariant J_2 are present. Furthermore it shows dependence on the Lode parameter for small stress triaxialities. For positive parameters $\omega > 0$ the void growth mechanisms are more dominant than for negative ones ($\omega < 0$). On the other hand, for large stress triaxialities the onset of damage is caused by void growth mechanisms only, therefore, $\beta = 0$.

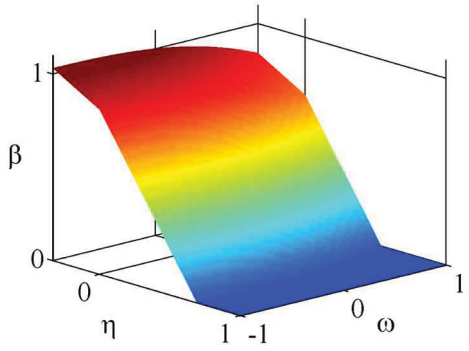

Figure 3: Damage mode parameter β vs. stress triaxiality η and Lode parameter ω

Furthermore the parameters $\bar{\alpha}$, $\bar{\beta}$ and $\bar{\delta}$ appearing in the damage rule (7) have been identified. The parameter $\bar{\alpha}$ (Fig. 4) is large for high positive stress triaxialities, small for moderate ones and negative for negative stress triaxialities. This means that for large stress triaxialities the damage behavior is dominated by isotropic growth of micro-voids. Dependence on the Lode parameter ω has not been numerical predicted by the simulations on the micro-scale.

$$\bar{\alpha}(\eta) = \begin{cases} -0.08197 + 0.80411\,\eta & \text{for } \frac{-1}{3} \leq \eta \leq 1 \\ 0.49428 + 0.22786\,\eta & \text{for } 1 < \eta \leq 2 \\ 0.87500 + 0.0375\,\eta & \text{for } 2 < \eta \leq \frac{10}{3} \\ 1 & \text{for } \eta > \frac{10}{3} \end{cases} \tag{16}$$

The Parameter $\bar{\beta}$ is given by the relation

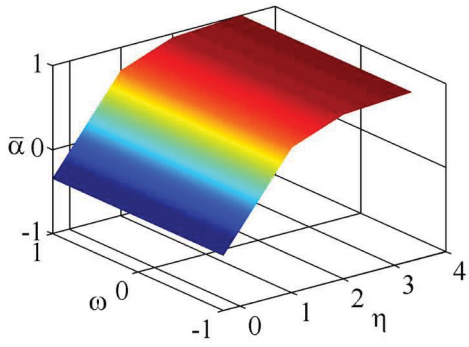

Figure 4: Damage strain rate parameter $\bar{\alpha}$ vs. stress triaxiality η and Lode parameter ω

$$\bar{\beta}(\eta,\, \omega) = \bar{\beta}_0(\eta) + f_\beta(\eta)\; \bar{\beta}_\omega(\omega) \tag{17}$$

with

$$\bar{\beta}(\eta,\,\omega) = \begin{cases} 0.94840 + 0.11965\,\eta + (-0.0252 + 0.0378\,\eta)(1-\omega^2) & \text{for } \frac{-1}{3} \le \eta \le \frac{1}{3} \\ 1.14432 - 0.46810\,\eta + (-0.0252 + 0.0378\,\eta)(1-\omega^2) & \text{for } \frac{1}{3} < \eta \le \frac{2}{3} \\ 1.14432 - 0.46810\,\eta & \text{for } \frac{2}{3} < \eta \le 2 \\ 0.52030 - 0.15609\,\eta & \text{for } 2 < \eta \le \frac{10}{3} \\ 0 & \text{for } \eta > \frac{10}{3} \end{cases} \tag{18}$$

which characterizes the amount of anisotropic isochoric damage strain rates caused by evolution of micro-shear-cracks. Figure 5 shows $\bar{\beta}$ as a function of the stress triaxiality and the Lode parameter. The parameter $\bar{\beta}$ is large for negative and low positive stress triaxialities, smaller for moderate ones and zero for high triaxialities. The negative and low positive triaxiality regimes show dependence on the Lode parameter which has been detected by the numerical simulations on the micro-scale. This influence has been considered by $\bar{\beta}_\omega(\omega)$ in Eq. (17). Only the parameters $\bar{\alpha}$ and $\bar{\beta}$ are not adequate enough to simulate

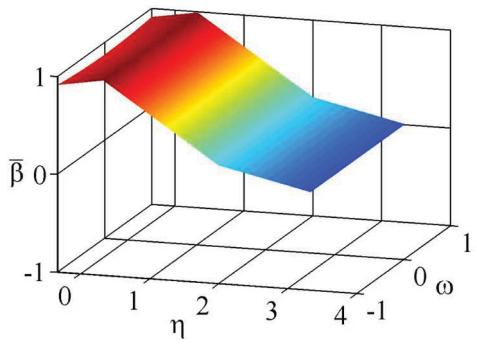

Figure 5: Damage strain rate parameter $\bar{\beta}$ vs. stress triaxiality η and Lode parameter ω

the macroscopic inelastic deformation behavior. According to this, the parameter $\bar{\delta}$ has to be taken into account to model in addition to $\bar{\beta}$ the formation of micro-shear-cracks:

$$\bar{\delta}(\eta,\,\omega) = f_\delta(\eta)\,\bar{\delta}_\omega(\omega) \tag{19}$$

with

$$\bar{\delta}(\eta,\,\omega) = \begin{cases} (-0.12936 + 0.19404\,\eta)(1-\omega^2) & \text{for } \frac{-1}{3} \le \eta \le \frac{2}{3} \\ 0 & \text{for } \eta > \frac{2}{3} \end{cases} \tag{20}$$

The parameter $\bar{\delta}$ is zero for large stress triaxialities and in comparison to $\bar{\alpha}$ and $\bar{\beta}$ small for small stress triaxialities but neglecting it leads to errors up to 20% in the macroscopic damage strain rates. It also shows dependence on the Lode parameter. With

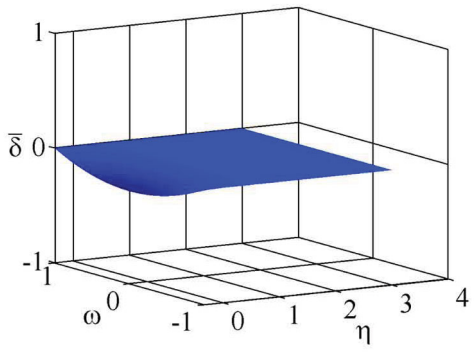

Figure 6: Damage strain rate parameter $\bar{\delta}$ vs. stress triaxiality η and Lode parameter ω

those functions it is possible to simulate with the continuum damage model the damage behavior predicted by the micro-mechanical simulations and, therefore, they can be interpreted as quasi experimental data. Figure 7 shows the comparison of different damage strain components for different loading conditions: in red predicted by the continuum damage model and in blue obtained by unit-cell analyses. Excellent agreement is given for negative, moderate as well as for large positive stress triaxialities and different Lode parameters. Therefore, all basic damage mechanisms (Fig. 1) can be taken into account by the continuum damage model in a phenomenological way. Altogether, the differences in Fig. 7 are marginal and the results demonstrate the accuracy of the continuum model for various stress triaxialities and Lode parameters.

5 CONCLUSIONS

The main objective of this paper is to give a short overview of the influence of stress state on damage and failure behavior of ductile metals. Thus, a contiuum damage model has been introduced taking into account the effect of stress intensity, stress triaxiality and the Lode parameter on constitutive damage equations. Basic material parameters have been determined by using experimental results from various uniaxial tests with differently notched tension and shear specimens. Additional series of three-dimensional numerical analyses on the micro-level covering a wide range of stress triaxialities and Lode parameters in the tension, shear and compression domains have been performed to get more information on the complex stress-state-dependent damage behavior. These results have been used to get more insight in the different damage mechanisms, to develop constitutive equations of the contiuum damage model as well as to identify stress-state-dependent parameters appearing in these equations. For high stress triaxialities no dependence on the Lode parameter could be detected but it could not be neglected for moderate or negative stress triaxialities. After all, the accuracy of the continuum model has been demonstrated by comparison of numerical results with data from the unit cell calculations for different loading conditions.

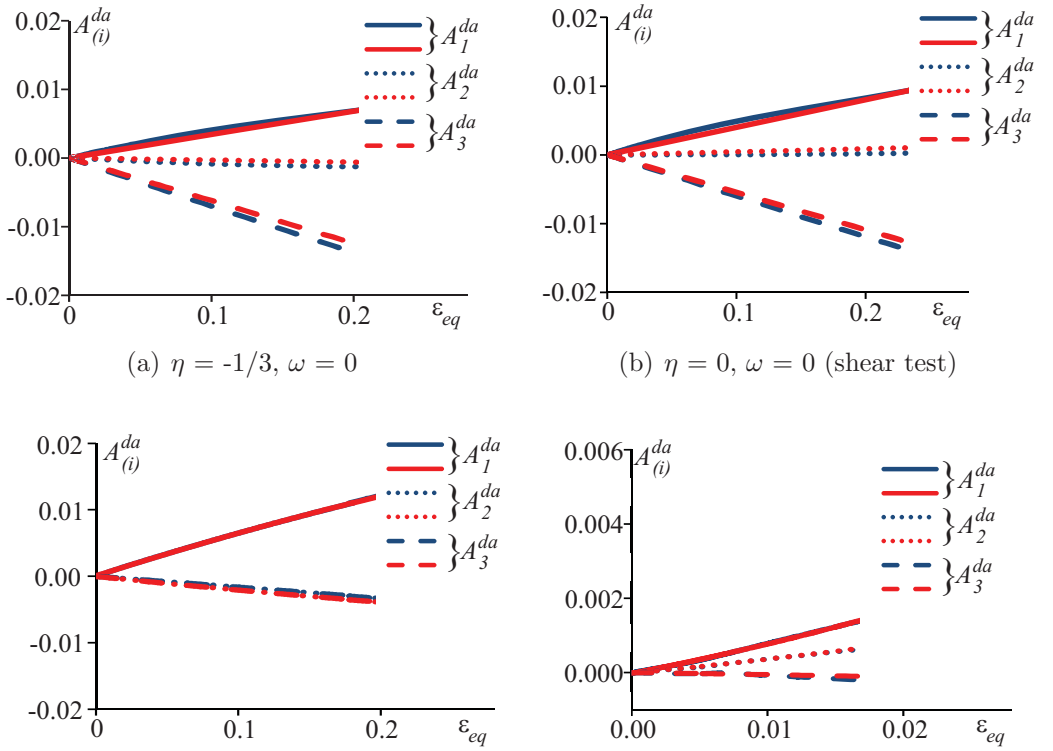

(a) η = -1/3, $\omega = 0$

(b) $\eta = 0$, $\omega = 0$ (shear test)

(c) $\eta = 1/3$, ω = -1 (tension test)

(d) $\eta = 1$, $\omega = 0$

Figure 7: Damage strain components vs. equivalent strain: Numerical results from the macroscopic model (red) and unit cell calculations (blue)

REFERENCES

[1] T. Børvik, O. S .Hopperstad, and T. Berstad, On the influence of stress triaxiality and strain rate on the behaviour of a structural steel. part ii. numerical study. *European Journal of Mechanics A/Solids*, **22**:15–32, 2003.

[2] Y. Bao and T. Wierzbicki, On the fracture locus in the equivalent strain and stress triaxiality space. *International Journal of Mechanical Sciences*, **46**:81–98, 2004.

[3] N. Bonora, D. Gentile, A. Pirondi, and G. Newaz, Ductile damage evolution under triaxial state of stress: theory and experiments. *International Journal of Plasticity*, **21**:981–1007, 2005.

[4] Y. Bai and T. Wierzbicki, A new model of metal plasticity and fracture with pressure and Lode dependence. *International Journal of Plasticity*, **24**:1071 – 1096, 2008.

[5] M. Brünig, O. Chyra, D. Albrecht, L. Driemeier, and M. Alves, A ductile damage criterion at various stress triaxialities. *International Journal of Plasticity*, **24**:1731–1755, 2008.

[6] X. Gao, T. Zhang, M. Hayden, and C. Roe, Effects of the stress state on plasticity and ductile failure of an aluminum 5083 alloy. *International Journal of Plasticity*, **25**:2366 – 2382, 2009.

[7] M. Brünig, D. Albrecht, and S. Gerke, Numerical analyses of stress-triaxiality-dependent inelastic deformation behavior of aluminum alloys. *International Journal of Damage Mechanics*, **20**:299–317, 2011.

[8] A. Needleman, Void growth in an elastic-plastic medium. *Journal of Applied Mechanics*, **39**:964–970, 1972.

[9] R. Becker, R.E. Smelser, and O. Richmond, The effect of void shape on the development of damage and fracture in plane-strain tension. *Journal of the Mechanics and Physics of Solids*, **37**:111 – 129, 1989.

[10] M. Kuna and D.Z. Sun, Three-dimensional cell model analyses of void growth in ductile materials. *International Journal of fracture*, **81**:235–258, 1996.

[11] K.S Zhang, J.B Bai, and D. Francois, Numerical analysis of the influence of the Lode parameter on void growth. *International Journal of Solids and Structures*, **38**:5847 – 5856, 2001.

[12] J. Kim, X. Gao, and T.S. Srivatsan, Modeling of crack growth in ductile solids: a three-dimensional analysis. *International Journal of Solids and Structures*, **40**:7357 – 7374, 2003.

[13] X. Gao, T. Wang, and J. Kim, On ductile fracture initiation toughness: Effects of void volume fraction, void shape and void distribution. *International Journal of Solids and Structures*, **42**:5097 – 5117, 2005.

[14] X. Gao, G. Zhang, and C. Roe, A study on the effect of the stress state on ductile fracture. *International Journal of Damage Mechanics*, **19**:75–94, 2010.

[15] M. Brünig, S. Gerke, and V. Hagenbrock, Micro-mechanical numerical studies on the stress state dependence of ductile damage. In: H. Altenbach and S. Kruch, *Advanced Materials Modelling for Structures*, Volume 19 of Advanced Structured Materials:87–96. Springer Berlin Heidelberg, 2013.

[16] M. Brünig, S. Gerke, and V. Hagenbrock, Micro-mechanical studies on the effect of the stress triaxiality and the Lode parameter on ductile damage. *International Journal of Plasticity*, **50**:49 – 65, 2013.

[17] M. Brünig, An anisotropic ductile damage model based on irreversible thermodynamics. *International Journal of Plasticity*, **19**:1679–1713, 2003.

[18] Y. Bao and T. Wierzbicki, On the cut-off value of negative triaxiality for fracture. *Engineering Fracture Mechanics*, **72**:1049–1069, 2005.

[19] A. S. Khan and H. Liu, A new approach for ductile fracture prediction on Al 2024-T351 alloy. *International Journal of Plasticity*, **35**:1 – 12, 2012.